SLD-Note-267
October 1999

Polarization measurement with the Quartz Fiber Calorimeter

D. Onoprienko

University of Tennessee, Knoxville, Tennessee 37996

Abstract

This note describes the Quartz Fiber Calorimeter (QFC) data analysis procedures, and presents the final results of the polarization measurement with the QFC. If you are only interested in the results, go straight to section 5 for the QFC versus SLD's standard CKV polarimeter comparison. The QFC systematic errors are summarised in table 2. Otherwise, read about the QFC data selection in section 1 (most of the cuts are identical to those used in the routine CKV data analysis). The algorithm for calculating the experimental asymmetry is described in section 2, which also discusses various sources of statistical errors. The study of systematics is presented in section 3.2. The transverse polarization measurement is beyond the scope of this note, but a brief summary can be found in section 4.

Contents

1 Polarimeter data selection

1.1 Procedure

The polarimeter acquires data at the SLC repetition rate of 120 Hz. The amount of data is very large - when all raw data is written to tape, the polarimeter accounts for approximately 20 % of all data logged by the SLD. In order to reduce the required tape space and facilitate the off-line analysis, the following procedure is adopted. The run is divided into $20,000$ events portions (each corresponding to approximately 3 minutes of uninterrupted running) called polruns. For each polrun, a summary data bank is produced containing the number of events, channel sums, and channel squared sums for each of the polarimeter channels. Only events that pass online cuts are used to accumulate the sums, and the data is accumulated separately for each of the laser and electron beam helicity states, as well as for the laser off state. Along with the channel sums, the summary data banks contain other information describing the state of the machine and the detector during the polrun, such as the data acquisition system settings, type of the calibration scan being performed, detector configuration and diagnostic parameters, etc. These data banks are written to tape and used in the mainstream polarimeter analysis.

Raw data is written to tape in separate data banks. During the normal running, only one of every 6 "laser off" events is written (which results in the equal

numbers of "laser on" and "laser off" events being logged). The data volume is therefore reduced by a factor of 7/2. When necessary, the data acquisition system can be configured to write all events. Raw data can be used whenever summary data is insufficient for the analysis - for example, for various systematic errors studies.

1.2 Online cuts

Four cuts are applied to the data online on event by event basis. To ensure that electrons are present in the machine, cuts are made on the electron toroid (signal should be above 45 ADC counts) and the electron dumper (flag should not be set). To exclude noisy pulses, the signal in the CKV channel 9 is required to be below 1000 ADC counts (this channel is beyond the kinematic edge of scattered electrons, and therefore provides a convenient measure of the beam related noise). Finally, the data acquisition system is required to be in a consistent state as reported by the SLC.

1.3 Offline cuts

The cuts applied to the summary data off-line on polrun by polrun basis are listed in table 1. They are designed to ensure data quality in both the QFC and the CKV detectors, and to exclude the CKV calibration polruns.

Table 1: QFC event selection off-line cuts.

Description	Value	Purpose
Number of events	> 400 in each of the four laser-on helicity states, $> 10,000$ background events.	Data quality.
Pockels Cell voltage	Nominal sequence, value within 50 V of nominal.	Exclude Pockels cell scans.
CKV PMT voltage	Within 2 V of nominal.	Exclude voltage scans.
CKV table position	Within 0.3 mm of nominal.	Exclude table scans.
CKV pre-radiator configuration	Nominal.	Data quality.
SLC reported status	Flag set by QBADPOL.	Data quality.
Compton laser status	Flag set by QLASDEF. Laser power setpoint is not below nominal.	Data quality. Exclude parts of laser power scans.
Electron toroid current	> 200 ADC counts.	Beam quality.
Positron toroid current	< 50 ADC counts.	Select electron only data.
CKV channel 7 mean signal size	$30 < signal < 250$, ADC counts.	Signal in linear range.
QFC vertical amplitude channel mean signal size	$50 < signal < 800$, ADC counts.	Signal in linear range, exclude noisy polruns.

1.4 Final data sample

Applying the cuts described above to the available electron-only data yielded a data sample equivalent to approximately 130 minutes of uninterrupted running. Most of the data (about 100 minutes) was taken during the QFC dedicated study in December 1997. This data sample was used for the final comparison between the results of the polarization measurements by the QFC and the CKV detectors.

In addition, substantial amount of the QFC calibration and systematics study data was taken throughout the SLD 1997 run, usually in parallel to normal SLD running or various machine studies.

2 Measuring experimental asymmetry

2.1 Asymmetry calculation

The first step in determining the polarization is to measure the asymmetry in the energy carried by the Compton photons, calculated between different electron-photon helicity combinations. Because the signs of both the laser and the electron beam polarizations are flipped randomly on event-by-event basis, and the laser only fires on every seventh machine pulse, we have six types of signals coming from the detector : S_{RR}, S_{RL}, S_{LR}, S_{LL}, S_{RO}, and S_{LO}, where the first subscript corresponds to the electron helicity (right or left), and the second subscript corresponds to the photon helicity(right, left, or laser off). The laser off events provide

a measure of the background seen by the detector. Figure 1 shows typical signal distributions for one of the QFC channels. The experimental asymmetry is formed as

$$A = \frac{S_{RL} + S_{LR} - S_{RR} - S_{LL}}{S_{RL} + S_{LR} + S_{RR} + S_{LL} - S_{RO} - S_{LO}} \tag{1}$$

Note that the asymmetry calculated in this way is a fairly robust quantity. While currents and polarizations of both the laser and the electron beams can have slight (less than 10^{-3}) left-right asymmetries, they automatically cancel out in the first order from the expression 1.

2.2 Statistical errors

This section discusses the statistical errors of the asymmetry measurement, which determine the time needed to achieve the desired accuracy. This in an important issue for the QFC polarimeter because the measurement cannot be performed in parallel to taking physics data with the SLD detector (to avoid huge background caused by beamstrahlung), and dedicated time has to be allocated for it. When the detector was first installed and tested, backgrounds in the amplitude channels exceeded the signal by more than two orders of magnitude, and the resulted statistical errors made a precise polarization measurement impossible. We used the SLD 1996 run to carry out a number of studies in order to identify the sources of the background and find a way to reduce it to acceptable levels. As a result, an

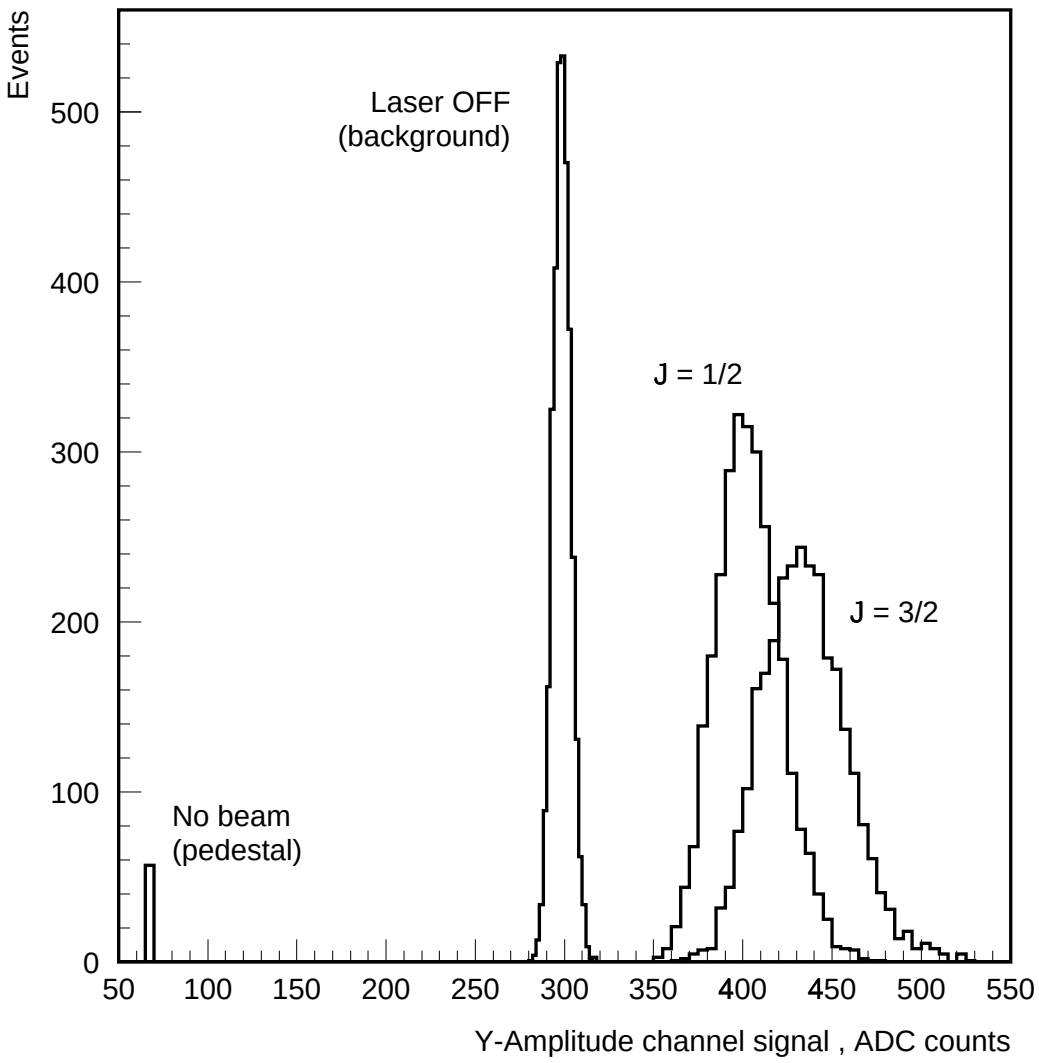

Figure 1: QFC signal distributions.

average statistical error in the measured polarization was reduced to about 2.5 % per 3 minute polarimeter run (about 20000 machine pulses), and was dominated by fluctuations in the effective luminosity of the electron and the photon beam collisions. This allowed for achieving our target accuracy of 0.5 % in less than 3 hours of data taking. The rest of this section describes the three major sources of statistical errors : background, pulse to pulse fluctuations in the number of Compton photons, and the QFC energy resolution.

2.2.1 Background

Overwhelming level of background observed during our first attempts to measure the beam polarization with the QFC forced us to undertake a detailed study of the background [1]. Two major sources of the background have been identified: scattered synchrotron radiation from the hard bend magnet, and a low energy halo around the beam produced by the beam tails in the upstream collimators and quadrupoles.

After passing the Compton interaction point, the electron beam is bent horizontally by a pair of dipole magnets, generating a high flux of synchrotron radiation. The first of the two magnets, the Soft Bend magnet, has a magnetic field of 0.385 kGauss and produces a deflection angle of 1.0 mrad, generating 462 TeV of synchrotron radiation per electron bunch (as compared to about 15 TeV energy carried by Compton photons) with a critical energy of 53.2 keV. This radiation,

as well as synchrotron radiation generated by the core of the electron beam in upstream quadrupoles, is effectively suppressed by the Čerenkov threshold of the quartz fibers (198 keV for electrons). The second dipole magnet, the Hard Bend magnet, has a field value of 11.69 kGauss and a bending angle of 17.3 mrad, producing $2.43 \cdot 10^5$ TeV of synchrotron radiation with a critical energy of 1.62 MeV. Due to the deflection of the electron beam by the Soft Bend magnet prior to the entry into the Hard Bend, there is 1 mrad separation between the direction of the neutral beam (Compton photons) and the beginning of the Hard Bend synchrotron stripe, which gives a 9 mm displacement at the location of the QFC detector.

Our original intention was to design and position the detector in a way that would ensure no scattering of the Hard Bend synchrotron stripe in the vicinity of the calorimeter. The absorber plates were shaped to let the Hard Bend synchrotron photons through without interaction. However, while this solution can be definitely used for the future e^+e^- colliders, it proved to be very difficult to implement for the SLD experiment, where the beam layout in the polarimeter area was not designed with a Compton photon detector in mind. Due to very limited space available for the QFC, it had to be placed near beam pipe flanges and a collimator, which scatter synchrotron radiation onto the detector. Our studies showed that this radiation was the major source of the background seen by the QFC. It was very stable, scaled with the electron beam current, and did

not depend on any other beam parameters.

The background produced by the Hard Bend synchrotron radiation was simulated [1] using the GEANT package. Comparison of the ratios of background signals in various types of the QFC channels between data and Monte Carlo confirmed that our simulation was fairly accurate. We then used it to optimize the shielding configuration around the detector. While the most efficient shielding concept would be to intercept the synchrotron stripe as far upstream from the QFC detector as possible, we were limited by the need to avoid creating additional backgrounds and possibly asymmetry contamination [2] for other detectors located in the area - most noticeably for the CKV detector. After extensive Monte Carlo study, we settled on a compromise configuration which allowed for achieving about 1:2 signal-to-background ratio in the amplitude channels - as compared to about 1:115 ratio observed during the SLD 1996 run.

The other source of the background was a low energy halo around the beam produced by the beam tails in the upstream collimators and quadrupoles. While being much smaller in magnitude than the background due to the scattered Hard Bend synchrotron radiation, this component was highly variable and contributed significantly to the statistical error of the polarization measurement. Since it was very sensitive to the beam steering, we were able to tune the beam to minimize the halo. Combined with tight shielding of all sides of the detector, especially of the transport fibers going from the calorimeter to the PMT box, beam tuning

allowed for almost complete elimination of this background component.

2.2.2 QFC energy resolution

The energy resolution of the QFC is determined by the shower fluctuations and the photoelectron statistics. Since the average total energy carried by the Compton photons in a single machine pulse is about 15 TeV, the requirements to the calorimeter energy resolution are fairy relaxed. Based on the beam test results which are in excellent agreement with Monte Carlo predictions, the resolution for 15 TeV of the incident energy (in the form of Compton photons in the 0 to 28.25 GeV energy range) is estimated to be 1.9 % for each of the amplitude channels.

2.2.3 Fluctuations in the energy carried by the Compton photons

The average total energy of the Compton photons generated per machine pulse is about 15 TeV. Taking into account the shape of the energy spectrum, this corresponds to approximately 3.6 % fluctuations in the total energy.

However, the dominating source of statistical errors is an uncertainty in the luminosity of the electron and the photon beams collisions caused by pulse to pulse fluctuations in the beams intensities, timing and position jitter. The size of this effect depends on the running conditions. For the data sample that was used for the QFC versus CKV comparison, the resulting fluctuations in the Compton

signal amplitude were about 17 % on the average.

3 Longitudinal polarization measurement

3.1 Analyzing power

The longitudinal polarization of the electron beam can be determined from the experimental asymmetries A_{amp} measured by the QFC amplitude channels using

$$P_e = \frac{A_{amp}}{P_\gamma a_{amp}} \tag{2}$$

with the analyzing power a_{amp} being equal, in the first approximation, the the asymmetry in the total energy carried by the scattered photons : $a^z_{amp} = 0.17332$. In order to account for the limited angular acceptance of the detector, finite beam size, and possible nonlinearity of the energy response function, the analyzing powers used in the analysis were deduced from the detailed Monte Carlo simulation of the calorimeter and surrounding beam line elements (see appendix B for details). The simulation yielded the following analyzing powers for the two QFC amplitude channels:

$$a^z_X = 0.17338$$

$$a^z_Y = 0.17366$$

where the subscripts X and Y mark the channels containing horizontal and vertical fibers respectively.

3.2 Systematic uncertainties

The summary of the QFC systematic errors is given in table 2 for the amplitude channels. Various sources of systematics are discussed in more details in the rest of this section.

3.2.1 Angular acceptance and the beam size

Since the angular divergence of the photon beam due to the Compton scattering is extremely small, the correction to the analyzing power caused by the limited angular acceptance of the detector is negligible (of the order of 10^{-5} for a point-like incident electron beam). Due to the real shape of the electron beam, the Compton spot size at the entry to the QFC is approximately 400 x 91 microns. This realistic beam size, together with the actual Compton photons angular distribution, were used in the Monte Carlo simulation. However, since the real beam parameters are not precisely known, we need to estimate the effect of an error in the beam size on the error in the QFC analyzing power. In order to do this, three beam configurations were simulated: point-like beam, realistic beam, and a round beam 800 x 800 microns (double size in horizontal direction). All three simulations yielded identical analyzing powers within 0.05 % - negligible effect compared to

Table 2: QFC: summary of systematic errors of the longitudinal polarization measurement. Numbers are given in per cent.

Calorimeter		
Angular acceptance, finite beam size	small	Compton cross section angular dependence, Monte Carlo simulation.
Energy response function linearity	0.2	Monte Carlo simulation, beam test.
Detector misalignment	0.1	Monte Carlo simulation, beam test.
Local non-uniformity	0.3	Monte Carlo simulation, beam test.
Optical cross talk	small	Measurement, Monte Carlo simulation.
Asymmetry contamination by re-scattered electrons	small	Monte Carlo simulation, *in situ* study.
Readout		
Readout linearity	0.5	LED study, beam test.
Electronic cross talk	0.1	*In situ* study.
Laser pickup	0.1	Direct measurement.
Total	0.6	

other sources of systematic uncertainties. The study assumed perfect alignment between the calorimeter and the beam. Possible effects of the position and angular misalignment are discussed below.

3.2.2 Energy response function

The relative difference between the theoretical analyzing power obtained by integration over the Compton spectrum, and the analyzing power determined by the Monte Carlo simulation, is 0.03 % and 0.19 % for the X-amplitude and Y-amplitude channels respectively. Since the effects of angular acceptance and finite beam size were found to be negligible, this difference is due entirely to the nonlinearity of the simulated energy response function (the dependence between the photon energy and the calorimeter response) of the detector, which could be caused by the shower leakages, Čerenkov threshold of the quartz fibers, and other effects. The energy response function was measured in the beam test in the 5-25 GeV range and found to be consistent with the Monte Carlo predictions (figure 2). However, since we did not check the response function in the whole range of possible Compton photon energies (from 0 to 28.25 GeV), we conservatively include the maximum deviation from the "theoretical" analyzing power observed in the simulation (0.2 %) in our estimate for the systematic error of the polarization measurement. Since the beam test was performed after the polarization measurements, the measured energy response function also included any effects

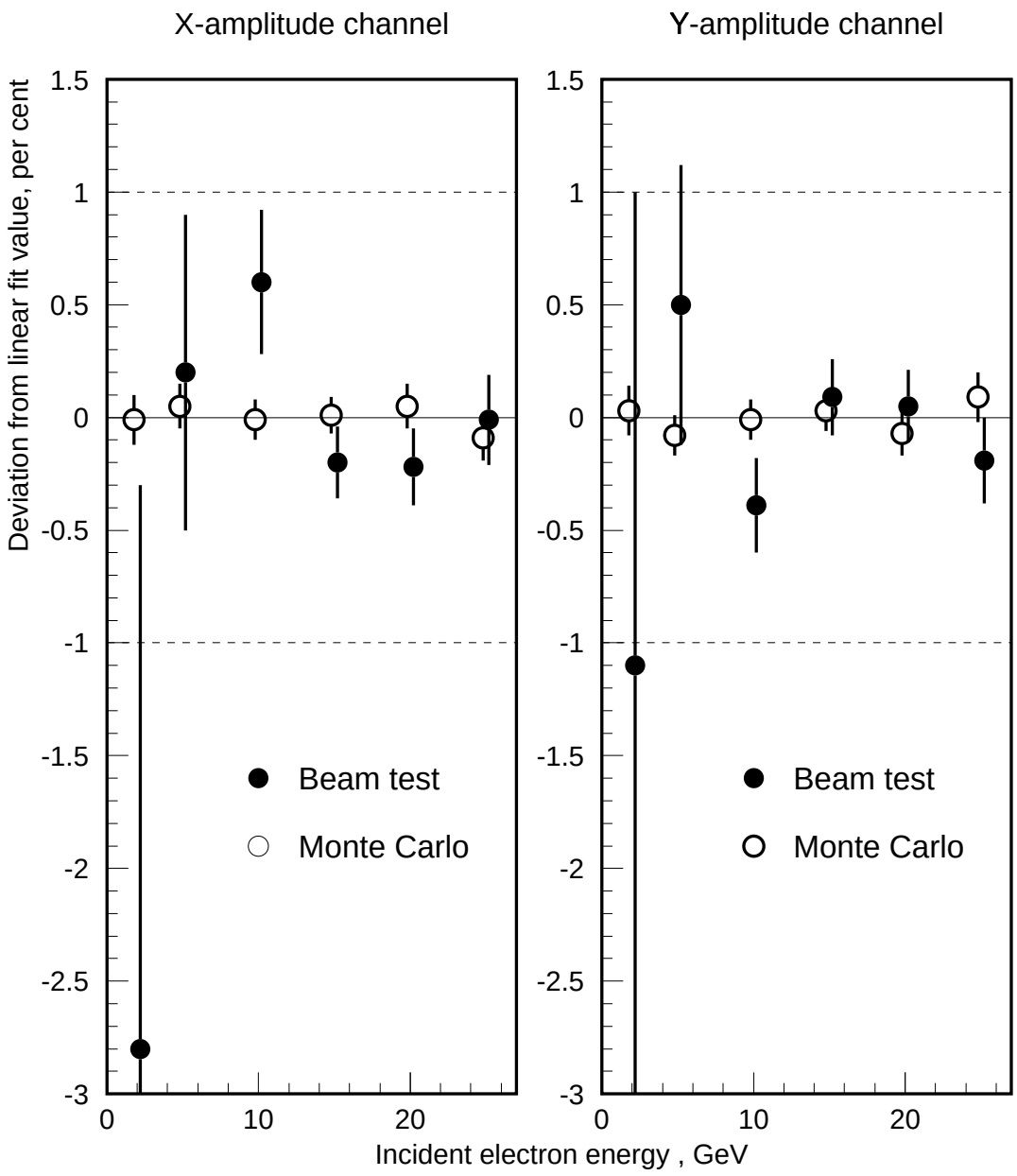

Figure 2: QFC energy response function: residuals to the linear fit.

of the possible radiation damage to the quartz fibers (even though we did not see any evidence of such damage).

3.2.3 Calorimeter misalignment

Survey data and the calorimeter's own position sensitivity allow for reliable determination of its position and angle with respect to the Compton beam with an accuracy of ± 100 microns and ± 0.7 degrees respectively (both are very conservative estimates, careful analysis of the information from the QFC coordinate channels allows for much better accuracy. However, there is no need to do this analysis for all the data). Within these limits, the effects of angular and position misalignment of the calorimeter with respect to the nominal beam line were studied both in Monte Carlo simulation and in the beam test. While we saw a sizeable effect of the angular misalignment on the asymmetry in coordinate channels, the asymmetry measured by the amplitude channels used for the longitudinal polarization measurement was unaffected at 0.1 % level.

3.2.4 Local non-uniformity in the calorimeter

We use the term "local non-uniformity" to describe deviations of the QFC real geometry from the nominal design due to mechanical tolerances associated with the calorimeter construction process. The nominal geometry was assumed in the Monte Carlo simulation that was used to calculate the analyzing powers. We

identified several categories of deviations from the nominal geometry that could in principle affect the measured asymmetry:

- fluctuations in the thicknesses of the absorber plates;
- misalignments between grooves in different absorber plates;
- uncertainty in the position of fibers inside the absorber groove (since the groove is slightly wider than the sum of outer diameters of all fibers inside it);
- fiber to fiber variations in the light attenuation length;
- uncertainty in the fibers path between the calorimeter and the phototube box.

All these categories were studied in Monte Carlo using the actual Compton beam parameters, and all except one were found to have negligible effects on the asymmetry in the amplitude channels. For these channels, the biggest potential problem is represented by the uncertainty in the fibers path between the calorimeter proper and the PMT box.

Since the fibers configuration in this "transport" region was only roughly known (fibers were attached to the calorimeter on one end, and to the phototubes on the other, but could follow any path in the middle, restricted only by the walls of the channel in shielding), we used the following method to obtain an

estimate for a systematic error associated with this uncertainty. The analyzing powers used in the analysis were generated using "nominal" fiber configuration in the transport region that represented our best educated guess. This nominal configuration was used for all other Monte Carlo studies. Six other configurations representing qualitatively different possible fibers paths in this region were also simulated. For each configuration, the signal generated in the fibers in the transport region and its asymmetry were estimated separately from the signal (and associated asymmetry) generated in the calorimeter proper. The results are listed in table 3. For the nominal geometry, the effect of the transport region signal on the total measured asymmetry was found to be very small (less than 10^{-4}). For all configurations, the portion of the signal generated in the transport region was in the range from 0.03 to 0.56 % of the total signal, while the relative difference between its asymmetry and the asymmetry in the total signal changed between -48.3 and +9.9 % of the total asymmetry. Combining the highest signal in the transport region with the highest asymmetry deviation, we obtain a conservative estimate of 0.3 % for the associated systematic error.

3.2.5 Optical cross talk

Since the fibers in each of the QFC longitudinal layers lie close to each other in the tungsten plate grooves, and all fibers follow the same path from the calorimeter to the phototube box, there is a chance that Čerenkov photons generated in one

Table 3: QFC: signal and asymmetry in the transport region between the calorimeter and the PMT box. The signal picked up by the fibers in the transport region is given in per cent of the total signal in the corresponding channel, for parallel helicities of the incident electrons and photons. Asymmetry deviation is the difference between the asymmetry of the transport region signal and the asymmetry of the total signal, in per cent of the total signal asymmetry. 100 % longitudinal polarization of the incident electron beam is assumed in the simulation.

Fiber path	X-amplitude channel			Y-amplitude channel		
	Signal	Asymmetry deviation	Effect on total asymmetry	Signal	Asymmetry deviation	Effect on total asymmetry
Nominal	0.26 %	+ 2.1 %	+ 0.01 %	0.19 %	+ 1.0 %	0.00 %
A	0.41 %	- 29.2 %	- 0.12 %	0.18 %	- 16.3 %	- 0.03 %
B	0.30 %	+ 8.1 %	+ 0.02	0.24 %	+ 0.9 %	0.00 %
C	0.11 %	- 48.3 %	- 0.06 %	0.03 %	- 39.6 %	- 0.01 %
D	0.56 %	+ 9.9 %	+ 0.05 %	0.39 %	+ 8.5 %	+ 0.03 %
E	0.23 %	-22.2 %	- 0.05 %	0.27 %	- 27.9 %	- 0.08 %

fiber can escape it and be captured by another fiber that belongs to a different channel, thus creating a cross talk. Our choice of clad fibers should make this effect very small. Simple test was done in order to verify this - a number of fibers were bundled together, and light from an LED source was sent through some of them. The fibers not connected to the light source were read out by a phototube, and the difference between the "LED ON" and "LED OFF" signals was measured. No cross talk was detected at 10^{-3} level, which implies completely negligible effect on the measured asymmetry since asymmetries in most fibers are close to each other.

3.2.6 Asymmetry contamination by re-scattered Compton electrons

Compton scattered electrons are analyzed by the CKV detector located on the opposite side of the beam pipe from the QFC. The electrons of different energies have different asymmetries ranging approximately from -0.26 to 0.75, and after going through a pair of dipole magnets, they are separated in space. Therefore, care should be taken to avoid re-scattering Compton electrons onto the QFC detector where they could contaminate the measured asymmetry. The problem was studied in Monte Carlo simulation, and no effect on the asymmetry was observed at 10^{-4} level. To confirm this conclusion experimentally, a portion of the data was taken with the CKV detector moved away from the beam.

3.2.7 Readout linearity

The linearity of the QFC readout was studied using the LED calibration system by measuring the dependence between the strength of the LED pulse and the ADC output. It was also checked in the beam test by looking at the dependence between the electron beam intensity (at a fixed energy) and the output signal. Both methods probe the response function of the complete readout chain including the phototube, the pre-amplifier, 60 meters long coaxial cable, and the ADC. Both have their limitations however: LED pulse shape is different from the pulse shape of the actual Compton signal, and the beam test data could be affected by nonlinearities in the response of the Čerenkov counter that was used to control the beam intensity (the counter was precisely calibrated by the E144 experiment so the effect should be small). For these reasons, we do not apply corrections associated with the measured electronics response function to the data, but rather include the effect of the observed deviation from linearity in our estimate for the systematic error. Consistency of the results obtained by two independent methods gives us confidence in the correctness of our estimate.

The QFC LED calibration system includes 7 LEDs. Any subset of these can be fired on any given data acquisition cycle. The light produced by the LEDs is picked up by 30 quartz fibers, each of which can be connected to a different QFC readout phototube. When all 7 LEDs are fired simultaneously, all fibers pick up

approximately equal amount of light (within 5 %). However, when only one of the side-mounted LEDs is fired, the amount of light in different fibers can differ by order of magnitude. This feature was utilized for the QFC readout linearity study. Several methods were used (determination of differential response function by measuring the response to a small light pulse on top of another light pulse of variable size, measuring the ratio of signals produced by light pulses of different strength while varying the high voltage settings, etc.) and produced consistent results. The most direct method is described below.

In this method, we chose an LED that produced signal in the channel being tested that was several times bigger than the signals produced in a few other channels ("control channels"), so that the whole dynamic range of the tested channel could be spanned while keeping the signal low in control channels. We then varied the LED pulse strength, and measured the signal in the tested channel as a function of the amount of light produced by the LED, as measured by control channels. Consistent results obtained with different sets of control channels and different LEDs confirmed that the measured response function was not significantly affected by nonlinearities in the control channels themselves. PMT gains were monitored throughout this study by simultaneously taking data with the center mounted LED that was sending approximately the same amount of light into each channel. The pulse strength of this LED remained unchanged, so it could be used to check the relative gains of the tested channel and the control

channels. Figure 3 shows an example of the measured response function for the X-amplitude channel. Residuals to the straight line fit are shown in figure 4. In order to calculate the effect on the measured asymmetry, the response function needs to be convoluted with the QFC signal distributions. For the data sample used for the QFC versus CKV comparison, the effect on the experimental asymmetry was found to be 0.1 ± 0.5 % for the X-amplitude, and 0.0 ± 0.4 % for the Y-amplitude channels.

In the beam test, we measured the QFC response as a function of the electron beam intensity, monitored by a calibrated Čerenkov counter. The measured dependence for the X-amplitude channel is shown in figure 5, and the residuals to the straight line fit are shown in figure 6. The corresponding effects on the measured Compton signal asymmetry are 0.3 ± 0.5 % for the X-amplitude, and -0.1 ± 0.5 % for the Y-amplitude channels.

3.2.8 Electronic cross talk

We used the Compton signal itself to study the effects of the electronic cross talk in order to ensure that the system was tested under exactly the same conditions as experienced during the actual polarization measurement. The effect was studied in two ways. First, we switched high voltage off for one of the QFC channels during normal data taking to see if there was any cross talk from the remaining 24 channels. Then, we switched off all channels but one to see if that channel

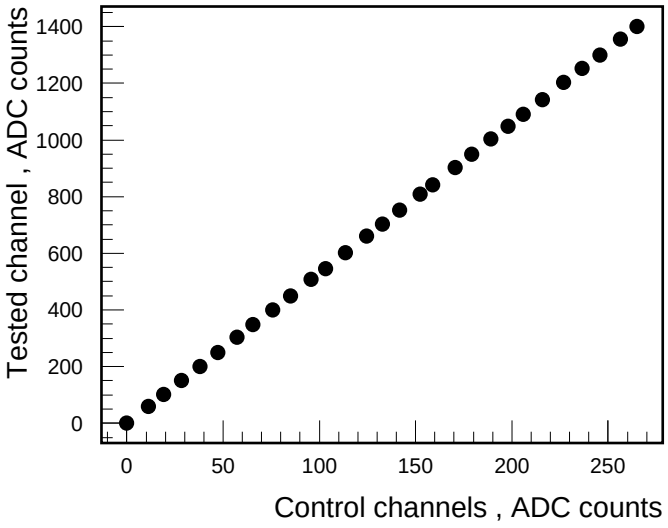

Figure 3: QFC readout linearity, LED test: X-amplitude channel response function. Signal in the tested channel as a function of the weighted average of the signals in control channels, pedestals are subtracted.

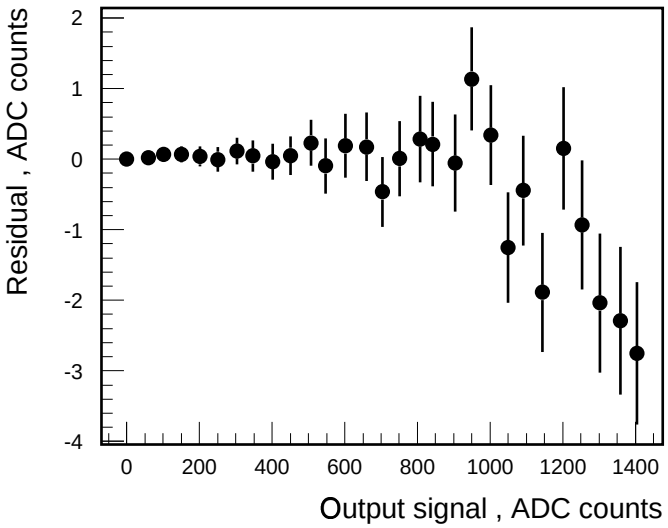

Figure 4: QFC readout linearity, LED test: X-amplitude channel response function, residuals to the linear fit.

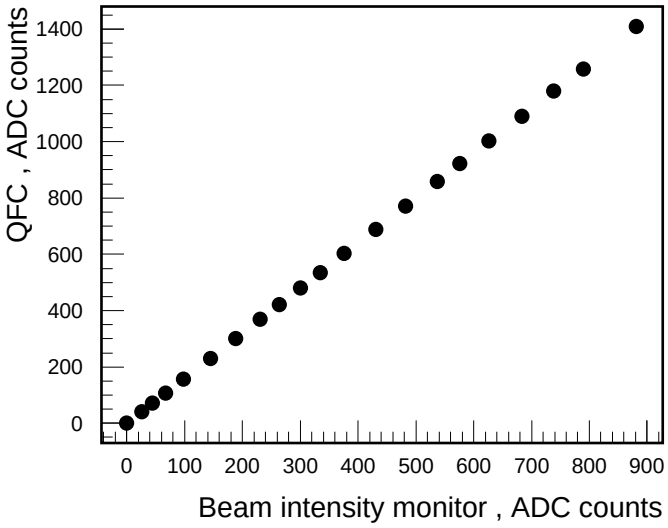

Figure 5: QFC readout linearity, beam test: X-amplitude channel response function. Signal in the tested channel as a function of the beam intensity measured by a calibrated Čerenkov counter, pedestals are subtracted.

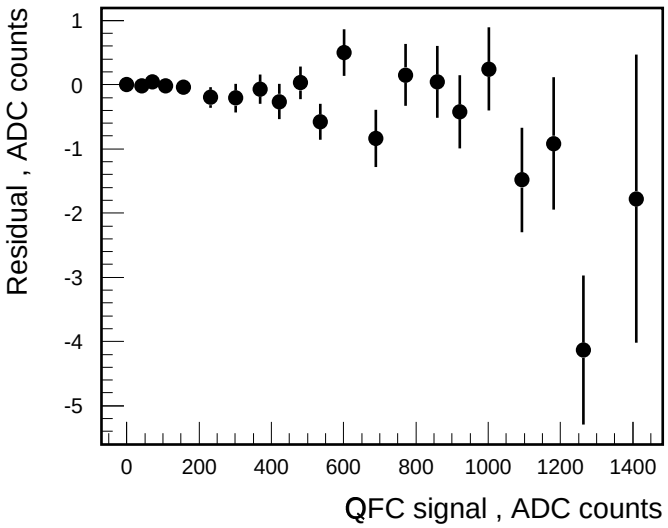

Figure 6: QFC readout linearity, beam test: X-amplitude channel response function, residuals to the linear fit.

created any cross talk in the other channels. The study was repeated for all QFC channels. Both methods showed no effect at the 0.1 ADC counts level - which corresponds to less than 0.1 % effect on the measured asymmetry in the amplitude channels.

3.2.9 Laser pickup

The QFC readout electronics is located in the outer room of the Compton laser shack. Since the electronics is not perfectly isolated from the laser room, very fast high voltage pulses of the laser Q-switch can generate small signals in the polarimeter readout channels. This effect is known as a "laser pickup" and requires some small corrections to be applied to the asymmetry measured by the polarimeter.

In the normal course of the SLC running, there are always machine pulses with no electron beam present in the Final Focus. Such pulses are identified by the requirement that the electron toroids signals should be less than 35 ADC counts above pedestal (normal beam-on signals are about 400 ADC counts) and the signals in all CKV channels should be less than 70 ADC counts above pedestal. The difference between "LASER ON" and "LASER OFF" signals for no-beam pulses provides a measure of the laser pickup.

We found that for the QFC detector, the laser pickup was time dependent, and was in the range between 0 and -0.1 ADC counts for most channels, including

amplitude channels, under normal running conditions. For a typical Compton signal in these channels (about 120 ADC counts, background subtracted), the effect on the measured asymmetry was a little less than 0.1 %.

For the data sample used for the QFC versus CKV comparison, the measured laser pickup is -0.05 ADC counts for the horizontal amplitude channel, and -0.06 ADC counts for the vertical amplitude channel. The corresponding corrections of -0.03 % and -0.05 % respectively are applied to the measured asymmetries. Since the machine pulses used to estimate the laser pickup are not the same pulses used for the polarization measurement, we conservatively associate an additional 0.1 % systematic error with this effect.

3.2.10 Beam optics configuration effects

The bulk of the QFC data used for the QFC versus CKV comparison was taken in the "narrow beam" mode - currents in two of the North Final Focus quadrupoles were scaled down to provide for a narrower beam through the Final Focus and reduce the QFC background. While the effect of this change on the QFC amplitude channels analyzing powers was apparently negligible (see section 3.2), the CKV measurement could in principle be affected since the spectrometer response function was somewhat sensitive to the beam size, and the Compton edge could move as a result of changes in the beam optics. The analyzing power tracking procedure based on monitoring the ratio of the signals in the CKV channels 6 and

7, which is routinely used in the CKV analysis, should automatically compensate for any such changes [3]. Comparing the results obtained in the two different beam modes can be used to verify this. Figure 7 shows the results of the polarization measurements by three CKV and two QFC channels for the data sample used for the CKV versus QFC comparison, calculated separately for the data taken in the "narrow beam" and the "nominal beam" modes. Since the data were taken on different dates, the difference in the absolute values of the measured polarization is expected. One important conclusion is that the observed discrepancy between the CKV channels 5, 6, and 7, is unrelated to the beam optics effects.

4 Transverse polarization measurement

Detailed description of the transverse polarization measurement with the QFC detector is outside the scope of this thesis since it is irrelevant to the A_{LR}^0 measurement. We expect to complete the analysis and publish a technical note describing the transverse polarization measurement in the future. In this section, we will only briefly discuss our experience and conclusions in this regard.

While we saw sufficient evidence that the detector is indeed sensitive to the transverse polarization, precise measurement based on the data taken during the SLD operation is hardly possible, due to a combination of the following problems :

- high background;

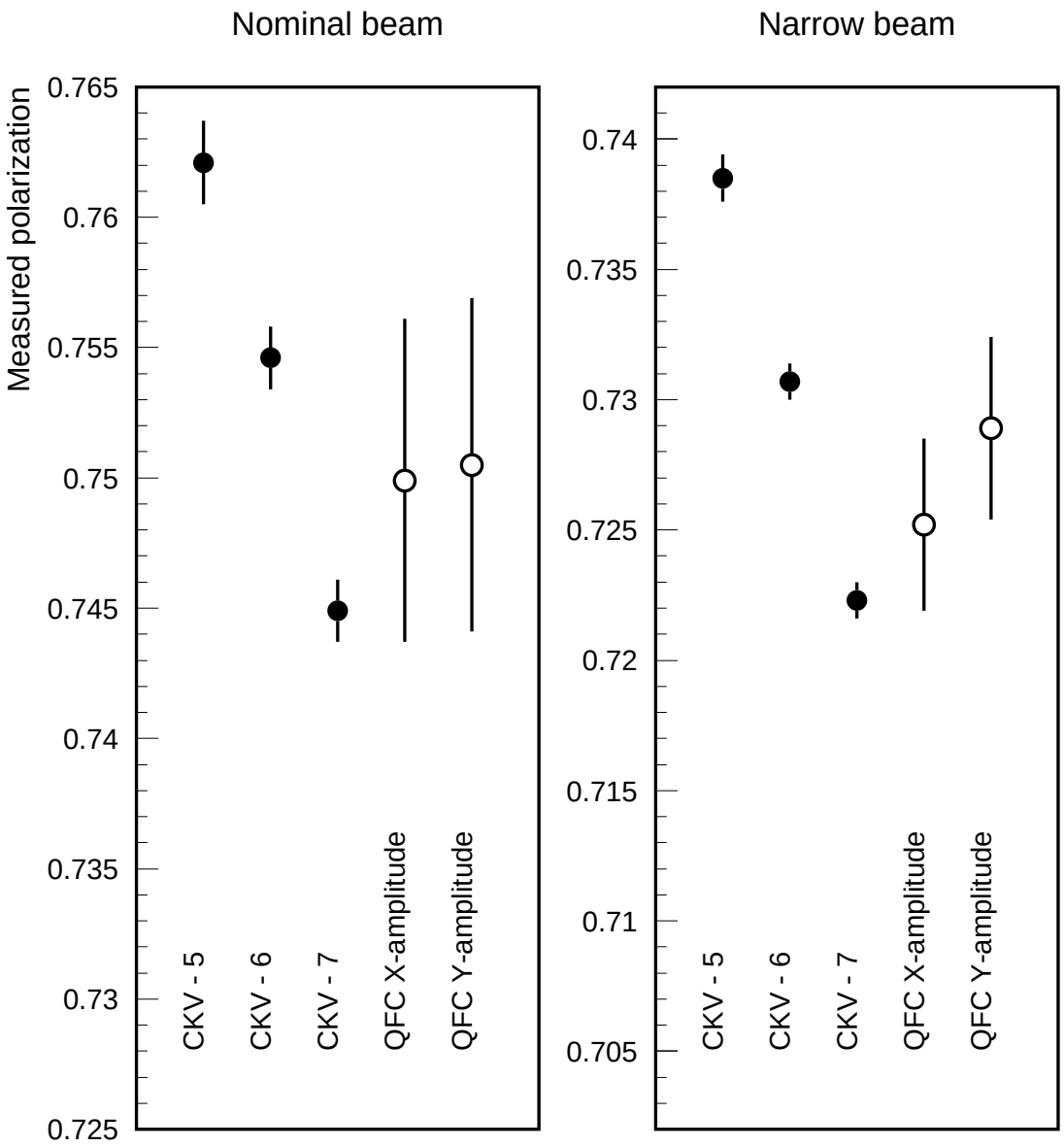

Figure 7: Polarization measurements with nominal and "narrow" beams. Errors shown are statistical only.

- lack of independent beam size information;
- beam position instability;
- lack of precise channel to channel calibration;
- limited space available for the detector, short distance to the Compton IP;
- problems with the beam quality during the QFC beam test.

The background radiation field in the detector area was not known until we studied it with the QFC. Our original scheme of the background suppression did not work because of very limited space available for the detector and unexpectedly high background from a low energy halo around the beam (see section 2.2.1 for details). Even with modified shielding configuration, signal-to-background ratio remained very low in the coordinate channels away from the shower axis. More important, making room for this modified shielding forced us to remove the remotely operated micrometer stage on which the calorimeter was originally mounted (the shielding could not be located further upstream from the detector because of concerns of creating additional backgrounds for other detectors located in the area). The stage would allow for both horizontal and vertical movements of the calorimeter, and transverse beam scans could be used for precise cross calibration of the QFC coordinate channels. Without the stage, we had to rely on the LED calibration system for channel to channel calibration which was only accurate to a few per cent. Since this was insufficient for a direct measurement of the position difference

between the Compton beams produced by the two electron-photon polarizations combinations (about 24 microns for a 100 % transversely polarized electron beam), we attempted to extract the transverse polarization by fitting the asymmetry distributions across the QFC channels. However, such asymmetry distributions were found to be sensitive to the detector angular misalignment and the size and shape of the incoming electron beam. Our ability to use the QFC itself to determine these parameters was negatively affected by the accuracy of the channel to channel calibration. We expected to have independent information on the electron beam parameters from the SLC instruments, but for the reasons not yet understood at the moment of this writing, a combination of the SLC measurements and simulations produced contradictory results for the beam configuration used during the polarization measurement with the QFC.

It should be noticed that all of the problems mentioned above can be either avoided or at least substantially reduced by designing the beam layout and the machine instrumentation from the ground up with the polarimeter in mind. This technology can certainly be used for transverse polarimeters at future collider experiments. However, keeping systematics under control is significantly more difficult than in the case of the longitudinal polarization. The longitudinal measurement using amplitude channels gets its power and low systematics from the fact that all geometrical effects (detector misalignment, local non-uniformity, beam size and shape uncertainties, etc.) cancel out from the measured asymmetry

in the first order, and the analyzing power of the detector is simply equal, to a few tenth of a per cent, to the integrated asymmetry in the Compton cross section. This is not the case for the coordinate channels that are used for the transverse polarization measurement.

5 Results

The polarization values measured by three CKV and two QFC channels for our final data sample are (statistical errors are listed first):

CKV channel 5 :	$P = 0.7442 \pm 0.0008 \pm 0.0076$
CKV channel 6 :	$P = 0.7364 \pm 0.0006 \pm 0.0053$
CKV channel 7 :	$P = 0.7277 \pm 0.0006 \pm 0.0027$
QFC X-amplitude channel :	$P = 0.7311 \pm 0.0029 \pm 0.0047$
QFC Y-amplitude channel :	$P = 0.7341 \pm 0.0031 \pm 0.0047$
QFC average :	$P = 0.7324 \pm 0.0029 \pm 0.0044$

Statistical errors in the two QFC channels are highly correlated. The systematic error estimates are based on the studies of relevant instrumental effects for each of the detectors. For the CKV polarimeter, the quoted systematic error does not include an additional uncertainty due to channel-to-channel inconsistency. Combining the measurements by different polarimeters allows for reduction of the final error of the measured polarization value used for physics analysis.

References

[1] William Bugg et al. The QFC polarimeter: Background problem. SLD-Note 255, Stanford Linear Accelerator Center, 1997.

[2] Dmitry V Onoprienko. Effect of scattering material in the neutral beam line on the asymmetry measured by the čerenkov Compton polarimeter. SLD-Note 254, Stanford Linear Accelerator Center, 1997.

[3] M. Fero et al. Compton polarization measurement: 1995. SLD-Physics-Note 50, Stanford Linear Accelerator Center, 1996.